Acta Crystallographica Section A
Foundations of Crystallography
ISSN 0108-7673

Received 8 January 2000
Accepted 31 January 2000

Evaluation of net atomic charges and atomic and molecular electrostatic moments through topological analysis of the experimental charge density

Anatoliy Volkov,[a] Carlo Gatti,[b] Yuriy Abramov[a] and Philip Coppens[a]*

[a]Department of Chemistry, State University of New York at Buffalo, Buffalo, NY 14260-3000, USA, and [b]Centro CNR-CSRSRC, Department of Physical Chemistry and Electrochemistry, University of Milano, via Golgi 19, 20133 Milano, Italy. Correspondence e-mail: coppens@acsu.buffalo.edu

The atoms in molecules (AIM) theory may be used to derive atomic charges, atomic volumes and molecular dipole moments from the charge density. The theory is applied to theoretical periodic Hartree–Fock (PHF), density-functional (DFT) and experimental X-ray densities of *p*-nitroaniline using the program *TOPOND* and a newly developed program, *TOPXD*, for topological analysis of densities described by the Coppens–Hansen multipole formalism. Results show that, like dipole moments derived directly from the multipole refinement, AIM-derived atomic and molecular moments are dependent on the multipole model used. As expected, large differences are found between charges derived from the monopole parameters and those from AIM analysis of the experimental model density. Differences between the κ'-restricted multipole model (KRMM) and the unrestricted multipole model (UMM) results are preserved in the AIM analysis. The enhancement of the molecular dipole moment of *p*-nitroaniline in the solid state is confirmed by both experiment and theory but the experimental dipole moment is in much better agreement with theoretical periodic Hartree–Fock and, especially, periodic DFT (PDFT) data when KRMM is used in the refinement. The AIM analysis allows a rigorous definition of the charges of the atoms in molecules and provides a realistic basis for comparison between molecules and between experiment and theory.

1. Introduction

The evaluation of atomic charges and molecule dipole moments from aspherical multipole refinements of experimental X-ray charge densities is subject to ambiguities resulting from overlap of the basis functions in adjacent molecules (Abramov *et al.*, 1999). It is therefore desirable to apply a method of electron-density partitioning that may be less sensitive to errors introduced by overlap of the basis sets. The atoms in molecules (AIM) theory of Bader (1990) defines a discrete rather than a fuzzy boundary on which space partitioning can be based. It is relatively basis-set independent compared to other methods, such as Mulliken population analysis and its variations. Thus, the AIM theory is an ideal tool for evaluation and comparison of properties of atoms and molecules. It is based on first principles and can equally well be applied to theoretical (both periodic and nonperiodic) and experimental charge densities. Although the AIM theory is quite computationally demanding, recent advances in computational technology have greatly reduced this drawback. At the current state of computer hardware development, computation of relatively large periodic systems (up to say 200 atoms in the unit cell) is quite feasible, and computing power is becoming less and less of a limitation. The AIM theory has been used to derive the experimental dipole moments of the water molecule in different environments (Flensburg & Larsen, 1999). A program capable of topological evaluation of bond critical-point parameters and the Laplacian of the electron density has been described recently (Souhassou & Blessing, 1999). But software for the routine evaluation of atomic and molecular properties from experimental charge densities using the AIM theory is not yet available.[1]

In order to fully incorporate the AIM analysis into routine X-ray charge-density studies, we have interfaced the existing program *TOPOND98* (Gatti, 1999) to the experimental charge-density package *XD* (Koritsanszky *et al.*, 1997). While the evaluation of charge-density properties at the critical

[1] After this work was completed, a paper describing a program for topological analysis of the density described by the *VALRAY* model was published (Flensburg & Madsen, 2000). We are grateful to one of the referees for pointing out the appearance of this paper.

points is included in *XD*, the main feature of the new program, *TOPXD*, is its capability to define atomic basin boundaries and integrate density functions within the basins, thus producing an extensive set of atomic properties, including net charges, dipole and higher electrostatic moments.

In the work described in this paper, the topological evaluation of atomic and molecular properties is applied to *p*-nitroaniline (PNA), using a set of 20 K synchrotron X-ray data collected at the National Synchrotron Light Source. Results are compared with those obtained from AIM analysis of theoretical single-molecule and periodic crystal wave functions obtained at Hartree–Fock (HF) and density-functional (DFT) levels.

2. Experimental data and refinements

Accurate 20 K X-ray data for PNA ($P2_1/c$) (Fig. 1) were collected at the SUNY X3A1 beamline at the NSLS ($\lambda = 0.643$ Å), using a closed-cycle helium Displex CT211 cryostat and a Bruker Smart 1000 CCD area detector. Details of data collection and processing are as for *p*-amino-*p*′-nitrobiphenyl (Volkov *et al.*, 1999). The crystal structure of PNA contains sheets of head-to-tail N—O···H—N hydrogen-bonded molecules, oriented parallel to the (101) plane.

Aspherical atom refinements were carried out with the *XD* package (Koritsanszky *et al.*, 1997), which uses the Hansen–Coppens multipole formalism (Hansen & Coppens, 1978; Coppens, 1997), following a recently described procedure (Abramov *et al.*, 1999). At the final stage, both standard unrestricted (UMM) and κ'-restricted (KRMM) multipole refinements were carried out. With UMM, all structural and electronic parameters are refined, while with KRMM the radial contraction/expansion coefficients (κ') are fixed at values derived from multipole refinements of theoretical structure factors on a number of compounds using periodic Hartree–Fock (PHF) calculations at the 6−21G** level (Abramov *et al.*, 1999). This approach imposes additional locality constraints on the atomic charge distribution and results in a more consistent representation of molecular dipole moments and superior deformation density maps. Full details on this method will be published elsewhere (Volkov, Abramov & Coppens, 2000). The AIM analysis was performed with the *TOPXD* program.

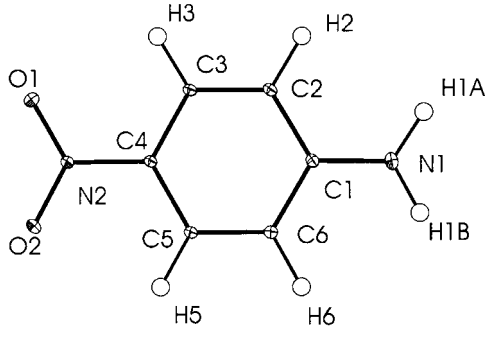

Figure 1
ORTEP plot of the PNA molecule.

3. Theoretical calculations

Single-molecule calculations were carried out at Hartree–Fock, density-functional and second-order Møller–Plesset perturbation-theory (Møller & Plesset, 1934) (MP2) levels using the *GAUSSIAN94* (Frisch *et al.*, 1995) program. DFT calculations were performed using Becke's (1988) functional, which includes Slater exchange along with corrections involving the gradient of the density, combined with Perdew & Wang's (1992) gradient-corrected correlation functional. In all isolated molecule calculations, the standard molecular split-valence 6−311G** basis set was used (Krishnan *et al.*, 1980).

Fully periodic calculations were performed with the *CRYSTAL98* program (Saunders *et al.*, 1998) at the Hartree–Fock (PHF) and DFT (PDFT) levels, the latter using the same exchange and correlation functionals as in the single-molecule calculations. All periodic calculations employed the split-valence 6−31G** basis set, modified as described in a previous paper (Abramov *et al.*, 2000).[2] Analysis of the theoretical electron density was performed with the programs *AIMPAC* (Biegler-König *et al.*, 1982; *AIMPAC*, 1997) and *TOPOND98* (Gatti, 1999) for single-molecule and periodic calculations, respectively.

Static crystal structure factors are obtained through Fourier transform of the ground-state charge density. In order to simulate the X-ray diffraction data, theoretical structure factors generated from both PHF and PDFT calculations included reflections within the range $0 < \sin\theta/\lambda < 1.05$ Å^{-1}. Since all reflections in this range were included, the number of theoretical structure factors exceeds the number of significant experimental observations. As for the experimental structure factors, all multipole refinements were carried out with the *XD* program and were based on *F*. However, no atomic temperature parameters were refined with the static theoretical data and all positional parameters were fixed. The UMM was used throughout, as in the KRMM the κ' parameters are already based on the theoretical density. *TOPXD* was used for the AIM analysis of the theoretical charge densities from the refinement.

Details of the multipole refinement of the experimental and theoretical structure factors are given in Table 1.

4. Topological definition of properties and the accuracy of integration

The *TOPXD* program is briefly described in Appendix *A*. Within the AIM theory, an atomic property is evaluated as an integral of the form (Bader, 1990)

[2] In order to avoid severe numerical instabilities in the calculations with the standard 6−31G** set, the diffuse outermost Gaussian function of the hydrogen and carbon atoms were modified [the exponents were changed from 0.161 277 80 (H) and 0.168 714 4 (C) to 0.2 Bohr^{-1} for both atoms].

$$A(\Omega) = \int_{\Omega} \rho_A(\mathbf{r})\, \mathrm{d}\tau,$$

where $A(\Omega)$ is the value of the property density $\rho_A(\mathbf{r})$ averaged over the atomic basin Ω. Thus, the integrated electronic charge of an atom is defined as

$$N(\Omega) = \int_{\Omega} \rho(\mathbf{r})\, \mathrm{d}\tau,$$

where $\rho(\mathbf{r})$ is the electron density. The net atomic charge $q(\Omega)$ is the difference between the nuclear (Z_Ω) and electronic $N(\Omega)$ charges:

$$q(\Omega) = Z_\Omega - N(\Omega).$$

The first moment of an atom's electron distribution, the atomic dipole, which measures the displacement of the centroid of the negative charge of an atom from the position of its nucleus, is given by

$$\boldsymbol{\mu}(\Omega) = -\int_{\Omega} \mathbf{r}_\Omega \rho(\mathbf{r})\, \mathrm{d}\tau,$$

where $\mathbf{r}_\Omega$ is the radius vector with its origin at the nuclear position. The total dipole moment of the system (molecule) is calculated as a sum over the net charge contributions and the first moments of all atoms in the system (molecule):

$$\boldsymbol{\mu}_{\text{molecule}} = \sum_i \{q_i(\Omega)\mathbf{X}_i + \boldsymbol{\mu}_i(\Omega)\},$$

where $\mathbf{X}_i$ is the position vector of the nucleus i measured from an arbitrary origin in the case of a neutral molecule. The first term in the curly brackets represents the charge-transfer contribution and the second the contribution arising from polarization of each atomic density. The atomic basin of the nucleus Ω is defined as a region in space bounded by interatomic surfaces (IAS) that satisfy the boundary condition of zero flux (Bader, 1990):

$$\nabla\rho(\mathbf{r}) \cdot \mathbf{n}(\mathbf{r}) = 0 \quad \forall\, \mathbf{r} \in \text{surface},$$

where $\nabla\rho(\mathbf{r})$ is the gradient vector field of electron density and $\mathbf{n}(\mathbf{r})$ is the vector normal to the surface at $\mathbf{r}$. Interatomic (or zero-flux) surfaces (IAS), and thus atomic basins in general, can be very complicated in shape. In order to determine an atomic basin, it is necessary to first find and describe its boundaries. Although analytical expressions for the interatomic surfaces have been proposed in the literature (Popelier, 1994*b*; Cioslowski & Stefanov, 1995), the determination of the interatomic surfaces is in practice better achieved by using numerical approaches (Popelier, 1994*b*; Biegler-König *et al.*, 1982; Gatti, 1999). In *TOPOND* and *TOPXD*, interatomic surfaces may be obtained either following an indirect method (Keith, 1993; Gatti *et al.*, 1994; Popelier, 1998), which relies on the fact that a nucleus is the terminal point for all the gradient paths within its basin (Bader, 1990), or with a two-step procedure. The latter uses in the first step an automated but simplified version of the standard *PROAIM* approach (Biegler-König *et al.*, 1982), which is based on the numerical determination of a set of downhill gradient paths emanating from the bond critical point associated with each IAS. In the second step, the indirect method is used for those integration rays whose length was incorrectly determined in the first stage. The complete indirect method, although much more time consuming, has proven to work accurately, even when the IAS have a very complicated shape and/or when the atomic boundaries are composed of many IAS.

Table 1
Summary of multipole refinements of experimental and theoretical structure factors.

	Experiment		Theory	
	UMM	KRMM	PHF/6-31G**	PDFT/6-31G**
$N_{\text{reflections}}$	3094	3094	5943	5943
$N_{\text{reflections}}/N_{\text{parameters}}$	18.2	19.0	43.4	43.4
R_F (%)	1.51	1.54	0.69	0.79
max Δ/σ	1×10^{-2}	2×10^{-6}	1×10^{-3}	1×10^{-2}

The accuracy of the numerical determination of the IAS and of the integration within the associated atomic basin was measured in terms of the integrated atomic Lagrangian, $L(\Omega)$, defined as

$$L(\Omega) = -\tfrac{1}{4}\int_{\Omega} \nabla^2\rho(\mathbf{r})\, \mathrm{d}\tau,$$

a quantity that should vanish because of the atomic basin boundary conditions. In practice, an acceptable integration is reached when $L(\Omega)$ is not larger than 1×10^{-3} atomic units (a.u.) for second-row atoms and 1×10^{-4} a.u. for hydrogen atoms. Two other parameters can be used to measure the quality of integration. They are the sum of net atomic charges and the sum of atomic volumes, the latter for periodic systems only. The former must be very close to the total charge of the unit being integrated, while the atomic volumes summed over the unit cell of the periodic system must accurately reproduce the unit-cell volume.

The results of the integration of the atomic basins of PNA are given in Tables 2 and 3 for both the experimental and theoretical charge densities. In the experimental case, determination of the IAS and subsequent integration typically took 20 h per atom on an SGI Origin 2000 computer using an R10000 processor. Inspection of the tables shows the accuracy of the AIM integration to be quite good in all cases. The sum of the absolute values of $L(\Omega)$ over the 16 atomic basins is not larger than 4×10^{-3} a.u. and the total molecular charge is 0.004 e or smaller. The sum over the volumes of the atomic basins in the unit cell reproduces the unit-cell volume quite well, the largest error being as small as 0.3%. In general, the figures of merit of integration of the experimental and theoretical densities are quite similar. However, in order to obtain integration of a quality comparable to that of the theoretical analysis, a somewhat finer grid had to be used for the IAS determination of the experimental density. The integration of the experimental density is, however, much faster (up to a factor of ten) because of the smaller number of functions used in the multipole model.

Table 2
Net atomic charges derived from monopole populations $q(Pv)$ and from AIM analysis $q(\Omega)$ in the PNA molecule from experimental and theoretical charge densities.

	Experiment				Theory					
	UMM		KRMM		PHF/6-31G**			PDFT/6-31G**		
Atom	$q(Pv)$	$q(\Omega)$	$q(Pv)$	$q(\Omega)$	$q(\Omega)$	$q(Pv)$†	$q(\Omega)$‡	$q(\Omega)$	$q(Pv)$†	$q(\Omega)$‡
Average O1, O2	−0.22 (3)	−0.45	−0.21 (3)	−0.44	−0.60	−0.24 (1)	−0.52	−0.56	−0.20 (1)	−0.47
N1 (amino)	+0.15 (9)	−0.87	+0.07 (9)	−0.99	−1.52	−0.13(2)	−1.16	−1.28	−0.09(2)	−1.02
N2 (nitro)	−0.07 (5)	+0.18	−0.01 (4)	+0.29	+0.31	−0.05 (2)	+0.27	+0.38	−0.06 (2)	+0.32
C1	−0.09 (7)	+0.27	−0.16 (6)	+0.26	+0.62	−0.03 (2)	+0.43	+0.50	−0.14 (3)	+0.32
Average C2, C6	+0.01(5)	−0.04	−0.04 (5)	−0.05	+0.08	−0.08 (2)	−0.02	−0.02	−0.03 (3)	−0.07
Average C3, C5	−0.11 (5)	−0.07	−0.08 (5)	−0.07	+0.07	−0.12 (2)	−0.04	+0.02	−0.15 (3)	−0.06
C4	+0.07 (7)	+0.19	+0.04 (6)	+0.21	+0.30	+0.18 (2)	+0.29	+0.21	+0.14 (3)	+0.17
Average H1*A*, H1*B*	+0.14 (3)	+0.47	+0.15 (3)	+0.47	+0.52	+0.18 (1)	+0.47	+0.48	+0.18 (1)	+0.44
Average H2, H6	+0.08 (2)	+0.12	+0.11 (2)	+0.10	+0.01	+0.13 (1)	+0.08	+0.08	+0.14 (1)	+0.14
Average H3, H5	+0.08 (2)	+0.10	+0.11 (2)	+0.11	+0.07	+0.16 (1)	+0.12	+0.09	+0.15 (1)	+0.13
$\sum q(NO_2)$	−0.51	−0.72	−0.43	−0.57	−0.89	−0.53	−0.77	−0.74	−0.46	−0.62
$\sum q(NH_2)$	+0.43	+0.07	+0.37	−0.05	−0.49	+0.23	−0.22	−0.31	+0.27	−0.14
$\sum q$	−0.0001	+0.002	+0.0002	+0.003	−0.00003	+0.0001	+0.004	+0.003	+0.0001	+0.001
$\sum \lvert L(\Omega)\rvert$	–	4×10^{-3}	–	4×10^{-3}	2×10^{-4}	–	4×10^{-3}	4×10^{-3}	–	2×10^{-3}
$\lvert\mu\rvert$ (Debye)	16.1 (11)	15.5	12.4 (10)	11.9	11.2	11.4 (2)	11.3	11.8	11.2 (3)	11.5

† Multipole refinement of theoretical structure factors. ‡ AIM analysis of electron density from multipole refinement of theoretical structure factors.

5. Atomic charges and molecular dipole moments

As may be expected when two different partitioning schemes are used, large differences are found between charges derived from the monopole parameters and those from AIM analysis of the experimental model density, which will be referred to below as *monopole charges* and *AIM charges*, respectively. The most dramatic differences between the two definitions are observed for the nitrogen atom of the amino (N1) group. The AIM nitrogen atom of the amino group is highly negative (−0.87–−0.99 e), while the monopole charge is slightly positive (0.15–0.07 e). The opposite situation is observed for N2, which is almost neutral according to the multipole refinement but quite positive from AIM (0.18–0.29 e). When total charges of the functional groups are compared, a large difference is found for the amino group, for which the AIM charge is very small (−0.05–0.07 e), while the monopole charge is quite positive (0.37–0.43 e). The similar trend is observed in theory (both PDFT and PHF) when atomic AIM charges are compared to monopole charges from multipole refinements of the theoretical structure factors.

Comparison of UMM and KRMM results shows that differences in atomic charges and molecular dipole moments based on the population parameters persist in the AIM-derived properties. For example, in the case of the UMM, the nitrogen atoms of the amino (nitro) groups are assigned fewer (more) electrons in both the monopole and AIM definitions.

In previous work, we found that multipole refinement of theoretical structure factors introduces a bias in the topological properties of the charge density at the bond critical points (Volkov, Abramov, Coppens & Gatti, 2000). The same effect is present for the AIM atomic charges and volumes, which are significantly affected when the density is projected into the basis functions of the multipole model. The shifts of the bond critical points upon multipole refinement of the theoretical structure factors are illustrated in Fig. 2 for both PDFT and PHF. The shifts correlate with the changes in atomic charges and atomic volumes, for instance the boundary surfaces separating each of the oxygen atoms from N2 shift toward the oxygen nuclei, resulting in smaller atomic volumes and less-negative net charges for the O atoms. A drastic shift of boundary surfaces is observed, for example, for the amino nitrogen (N1), for which the IAS with all the three linked atoms move inwards by up to 0.1 Å, resulting in an N1-volume decrease as large as 1.2 $Å^{-3}$ and a charge that is less negative by 0.24–0.36 e.

The molecular dipole moments obtained from the experimental and theoretical charge densities are compared in Table 4. Despite the large differences between monopole-derived and AIM charges, the molecular dipole moments agree quite well when *XDPROP* (the properties evaluation code in *XD*) and *TOPXD* results are compared. This illustrates that the differences between the AIM and monopole

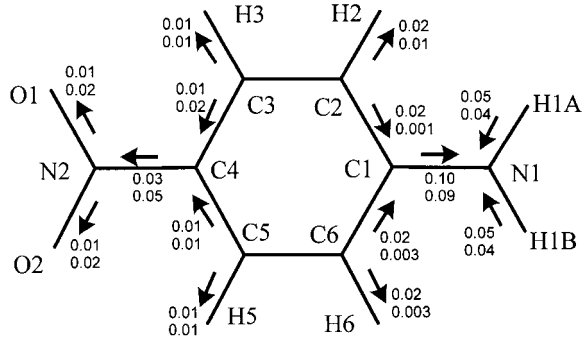

Figure 2
Effect of the multipole UMM on the position of the IAS in the theoretical charge density. First line: PHF, second line PDFT calculations. The arrows show directions and numbers represent distances (Å) of the shifts of the bond critical points.

Table 3
Atomic volumes (in Å^3) in the PNA molecule from AIM analysis of experimental and theoretical charge densities.

Calculated volume of the unit cell from cell parameters is 612.3 Å^3.

	Experiment		Theory			
			PHF/6-31G**		PDFT/6-31G**	
Atom	UMM	KRMM	TOPOND†	TOPXD‡	TOPOND†	TOPXD‡
O1	17.2	17.1	17.2	16.9	17.1	16.7
O2	17.2	17.2	17.5	17.2	17.4	17.1
N1 (amino)	17.3	18.0	19.8	18.6	18.7	17.9
N2 (nitro)	7.9	7.5	7.2	7.3	7.3	7.3
C1	8.9	8.8	7.7	8.2	8.1	8.5
C2	11.5	11.3	10.9	11.5	11.0	11.6
C3	11.5	11.4	10.6	11.4	10.8	11.4
C4	8.8	8.8	9.0	9.0	8.8	9.1
C5	10.9	10.8	10.2	10.6	10.4	10.8
C6	12.1	11.8	11.4	12.1	11.6	12.0
H1*A*	3.0	3.0	3.5	3.3	3.6	3.5
H1*B*	2.6	2.6	2.8	2.8	3.2	3.1
H2	5.6	5.7	6.4	5.7	6.2	5.5
H3	6.5	6.5	6.7	6.5	6.6	6.6
H5	5.2	5.3	5.3	5.2	5.4	5.2
H6	6.6	6.8	6.8	6.6	6.5	6.6
$V_{\rm AIM\ molecule}$ (Å^3)	152.6	152.6	152.9	152.7	152.8	152.8
$V_{\rm AIM\ unit\ cell}$ (Å^3)	610.6	610.6	611.8	610.9	611.3	611.3
$V_{\rm AIM\ unit\ cell}/V_{\rm calc}$ (%)	99.7	99.7	99.9	99.8	99.8	99.8

† Theoretical charge density. ‡ Charge density from multipole refinement of theoretical structure factors.

atomic charges are a result of the different partitioning schemes, rather than differences in the charge distribution. The same trend is observed in the theoretical analysis, *i.e.* the dipole moments from the multipole refinement of the theoretical structure factors and those from the *TOPXD* analysis of the density based on the same structure factors agree well with each other.

Both experiment and theory predict an increase in the molecular dipole moment of PNA upon crystallization, the theoretical (PHF and PDFT) and experimental values being 11.2–11.8 and 11.9–16.1 D, respectively, while the free-molecule value is 7.1 D according to MP2 and ~8.1 D according to the DFT and HF calculations. Table 4 also lists the components of the dipole-moment vector along the axes of the inertial coordinate system with its origin at the center of mass. The numbers show that the enhancement of the dipole moment of PNA in the solid state occurs mainly along the *X* axis, which is the long molecular axis. The directions of the dipole moments among all calculations agree well, the average error being as little as 1.0°. The largest disagreement in the direction of the $\boldsymbol{\mu}$ vector is 2.1° between single-molecule HF/6−311G** calculation and the AIM analysis of the electron density from multipole refinement of PHF/6−31G** structure factors. HF and DFT calculations on the isolated molecule and the crystal suggest a change in the dipole moment of PNA upon crystallization that is similar in direction and magnitude (about 1.2°).

Not unexpectedly, the experimental KRMM dipole moment of PNA is in much better agreement with theoretical values than the conventional UMM moment, illustrating the importance of the choice of multipole model. The dipole moments from AIM analysis of the experimental KRMM and theoretical HF and PDFT densities are in excellent (and possibly fortuitous) agreement. Net AIM atomic charges from the different methods similarly agree well, especially when theoretical density is projected into the same multipole-density functions. Error analysis of the experimental AIM properties will be the subject of future studies.

6. Conclusions

The determination of molecular electrostatic properties through topological analysis of the molecular electron density is a logical extension of the aspherical atom multipole refinement. For *p*-nitroaniline, the AIM analysis of the experimental charge density produces dipole moments close to those obtained directly from the multipole population parameters. Differences between the KRMM and UMM results are preserved in the AIM analysis. Nevertheless, the AIM analysis, being based on first principles, gives a more rigorous definition of the charges of the atoms in molecules, thus providing a more reliable framework for comparison between molecules and between experiment and theory. The pronounced increase in the molecular dipole moment in the solid state relative to isolated molecule values, also found in previous studies (Howard *et al.*, 1992; Gatti *et al.*, 1994; Abramov *et al.*, 1999; Zhang & Coppens, 1999), is confirmed by all methods applied in our work.

APPENDIX *A*
The *TOPXD* program

TOPXD is a program for complete topological analysis of experimental charge densities based on the Hansen–Coppens multipole formalism. It is based on *TOPOND98* (Gatti, 1999), originally interfaced to the *CRYSTAL98* package (Saunders *et al.*, 1998), with subroutines for geometrical calculations and density evaluations rewritten in *XD* conventions. The entire code is written in standard Fortran77 and can be ported to virtually any computer system.

The main features of the program are those of *TOPOND98*, *i.e.* a fully automated chain-like search for critical points in ρ and $\nabla^2\rho$ fields, using either the conventional Newton–Raphson technique or the eigenvector following method

Table 4
Theoretical and experimental molecular dipole moments (Debye) in PNA.

Components of the dipole moments are in an inertial coordinate system with the origin at the center of mass.

	$\|\mu\|$	μ_X	μ_Y	μ_Z
Theoretical (free molecule in crystal geometry)				
HF/6-311G**†	8.2	8.2	0.0	0.1
DFT/6-311G**†	8.0	8.0	0.0	0.1
MP2/6-311G**†	7.1	7.1	0.0	0.1
Theoretical PHF/6-31G** (crystal)				
TOPOND†	11.2	11.2	0.2	0.0
UMM/*XDPROP*‡	11.4	11.4	0.3	0.2
UMM/*TOPXD*‡	11.3	11.3	0.4	0.2
Theoretical PDFT†/6-31G** (crystal)				
TOPOND†	11.8	11.8	0.2	-0.1
UMM/*XDPROP*‡	11.2	11.2	0.2	0.1
UMM/*TOPXD*‡	11.5	11.5	0.3	0.2
Experimental				
UMM/*XDPROP*‡	16.1(10)	16.1	0.1	0.2
UMM/*TOPXD*‡	15.5	15.5	0.2	0.2
KRMM/*XDPROP*‡	12.4(10)	12.4	0.2	0.2
KRMM/*TOPXD*‡	11.8	11.8	0.2	0.2

† AIM analysis of theoretical charge density. ‡ Model used in the refinement/program used for the derivation of properties.

(Baker, 1986; Popelier, 1994*a*), a grid search of critical points in the asymmetric unit, the evaluation of atomic properties and finely tuned algorithms for the evaluation of atomic interaction lines or of atomic graphs. Several graphic options (tracing of $\nabla\rho$ trajectories, molecular graphs *etc.*) will be added.

The experimental electron density and its analytical derivatives up to order 2 are calculated using subroutines from the *XD* package, slightly modified for optimal performance. However, derivatives of a higher order (up to 4) are required when searching for critical points in the field of the Laplacian of the electron density. Derivatives of third and fourth order are evaluated in *TOPXD* as a numerical finite-difference approximation of the first- and second-order analytical derivatives. For that purpose, well known central-difference expressions with fourth-order error $[O(h^4)]$ have been used (Gerald & Wheatley, 1989):

$$f'_x = \frac{-f_{x+2h} + 8f_{x+h} - 8f_{x-h} + f_{x-2h}}{12h} \quad (1)$$

$$f''_x = \frac{-f_{x+2h} + 16f_{x+h} - 30f_x + 16f_{x-h} + f_{x-2h}}{12h^2}, \quad (2)$$

where x is the point at which the numerical derivative is evaluated and h is the step size. Higher-order numerical derivatives are not needed because every derivative of order 2 to 4 can be represented as a first- or second-order finite-difference numerical approximation of the first- or second-order analytical derivative using a simple chain rule, for example:

$$\frac{\mathrm{d}^3\rho}{\mathrm{d}x^2\mathrm{d}y} = \frac{\mathrm{d}}{\mathrm{d}x}\left[\frac{\mathrm{d}^2\rho}{\mathrm{d}x\mathrm{d}y}\right] = \frac{\mathrm{d}}{\mathrm{d}y}\left[\frac{\mathrm{d}^2\rho}{\mathrm{d}x^2}\right] = \frac{\mathrm{d}^2}{\mathrm{d}x^2}\left[\frac{\mathrm{d}\rho}{\mathrm{d}y}\right],$$

in which expressions in square brackets are analytical derivatives while the outer part is evaluated numerically.

The accuracy of the numerical differentiation of the electron density has been extensively tested by comparison of the numerical first and pure second derivatives with those obtained analytically for a number of (3, −1) critical points and for some arbitrarily selected points. With a step size of $h = 5 \times 10^{-3}$, the expected error in the numerical derivatives is only $O(h^4) = 6.25 \times 10^{-10}$. Numerical examples show the actual error to be less than 1×10^{-9} and practically non-existent when double-precision variables are used. A comparison of analytical mixed second derivatives with those obtained by numerical finite-difference differentiation of the first analytical derivative shows the difference to be less than 1×10^{-9}. A drawback of numerical differentiation is that, in order to approximate one derivative, several evaluations of the function are required. Indeed, in order to obtain a numerical approximation of a pure second derivative, for example $\mathrm{d}^2\rho/\mathrm{d}x^2$ [equation (2)], evaluation of density is required at five different points with five different coordinates. Fortunately, owing to the exceptional computational power of modern computers, such evaluations are only slightly more costly than using pure analytical expressions.

We would like to thank Dr Matthew D. Jones for his help at the computational stage of this work. Support of this work by the National Science Foundation (CHE9615586) and the US Department of Energy (DE-FG02-86ER45231) is gratefully acknowledged. All theoretical calculations were performed at the Center for Computational Research at SUNY at Buffalo, which is supported by grant DBI9871132 from the National Science Foundation.

References

Abramov, Yu. A., Volkov, A. & Coppens, P. (1999). *Chem. Phys. Lett.* **311**, 81–86.
Abramov, Yu. A., Volkov, A., Wu, G. & Coppens, P. (2000). *J. Phys. Chem. B.* In the press.
AIMPAC (1997). McMaster University, Ontario, Canada.
Bader, R. F. (1990). *Atoms in Molecules: a Quantum Theory.* Oxford: Clarendon Press.
Baker, J. (1986). *J. Comput. Chem.* **7**, 385.
Becke, A. D. (1988). *Phys. Rev. A*, **38**, 3098.
Biegler-König, F. W., Bader, R. F. & Tang, T.-H. (1982). *J. Comput. Chem.* **13**, 317.
Cioslowski, J. & Stefanov, B. B. (1995). *Mol. Phys.* **84**, 707–716.
Coppens, P. (1997). *X-ray Charge Densities and Chemical Bonding.* New York: Oxford University Press.
Flensburg, C. & Larsen, S. (1999). XVIII IUCr Congress, Glasgow, Scotland, Abstract P06.13.017.
Flensburg, C. & Madsen, D. (2000). *Acta Cryst.* A**56**, 24–28.
Frisch, M. J., Trucks, G. W., Schlegel, H. B., Gill, P. M., Johnson, B. G., Robb, M. A., Cheeseman, J. R., Keith, T., Petersson, G. A., Montgomery, J. A., Raghavachari, K., Al-Laham, M. A., Zakrzewski, V. G., Ortiz, J. V., Foresman, J. B., Cioslowski, J., Stefanov, B. B., Nanayakkara, A., Challacombe, M., Peng, C. Y., Ayala, P. Y., Chen, W., Wong, M. W., Andres, J. L., Replogle, E. S., Gomperts, R., Martin, R. L., Fox, D. J., Binkley, J. S., Defrees, D. J., Baker, J.,

Stewart, J. P., Head-Gordon, M., Gonzalez, C. & Pople, J. A. (1995). *GAUSSIAN 94*, Revision E.2. Pittsburgh, PA, USA: Gaussian Inc.
Gatti, C. (1999). *TOPOND98 User's Manual.* CNR-CSRSRC, Milano, Italy.
Gatti, C., Saunders, V. R. & Roetti, C. (1994). *J. Chem. Phys.* **101**, 10686–10696.
Gerald, C. F. & Wheatley, P. O. (1989). *Applied Numerical Analysis.* Reading, MA: Addison-Wesley.
Hansen, N. K. & Coppens, P. (1978). *Acta Cryst.* A**34**, 909–921.
Howard, S. T., Hursthouse, M. B., Lehmann, C. W., Mallinson, P. R. & Frampton, C. S. (1992). *J. Chem. Phys.* **97**, 5616–5630.
Keith, T. A. (1993). PhD thesis, McMaster University, Ontario, Canada.
Koritsanszky, T., Howard, S., Su, Z., Mallinson, P. R., Richter, T. & Hansen, N. K. (1997). *XD – A Computer Program Package for Multipole Refinement and Analysis of Electron Densities from Diffraction Data.* Free University of Berlin, Germany.
Krishnan, R., Binkley, J. S., Seeger, R. & Pople, J. A. (1980). *J. Chem. Phys.* **72**, 650.
Møller, C. & Plesset, M. S. (1934). *Phys. Rev.* **56**, 618.
Perdew, J. P. & Wang, Y. (1992). *Phys. Rev. B*, **45**, 13244.
Popelier, P. L. A. (1994*a*). *Chem. Phys. Lett.* **228**, 160–164.
Popelier, P. L. A. (1994*b*). *Theor. Chim. Acta*, **87**, 465–476.
Popelier, P. L. A. (1998). *Comput. Phys. Commun.* pp. 180–190.
Saunders, V. R., Dovesi, R., Roetti, C., Causà, M., Harrison, N. M., Orlando, R. & Zicovich-Wilson, C. M. (1998). *CRYSTAL98 User's Manual.* University of Torino, Italy.
Souhassou, M. & Blessing, R. H. (1999). *J. Appl. Cryst.* **32**, 210–217.
Volkov, A., Abramov, Yu. & Coppens, P. (2000). In preparation.
Volkov, A., Abramov, Yu., Coppens, P. & Gatti, C. (2000). *J. Mol. Struct. (Theochem).* To be published.
Volkov, A., Wu, G. & Coppens, P. (1999). *J. Synchrotron Rad.* **6**, 1007–1015.
Zhang, Y. & Coppens, P. (1999). *Chem. Commun.* pp. 2425–2426.